THE JOURNAL OF PHYSICAL CHEMISTRY A

 VOLUME 106, NUMBER 48, DECEMBER 5, 2002

ARTICLES

Reorientational Dynamics of the Model Compound 1,2,3,4-Tetrahydro-5,6-dimethyl-1,4-methanonaphthalene in Neat Liquid from Temperature-Dependent ^{13}C Nuclear Magnetic Relaxation Data: Spectral Densities and Correlation Functions

Andreas Dölle*

Institut für Physikalische Chemie, Rheinisch-Westfälische Technische Hochschule, 52056 Aachen, Germany

Received: March 29, 2002; In Final Form: July 2, 2002

The reorientational motion of the hydrocarbon 1,2,3,4-tetrahydro-5,6-dimethyl-1,4-methanonaphthalene (5,6-Me_2THMN) was studied over a wide range of temperature by the evaluation of ^{13}C spin−lattice relaxation rates and NOE factors. The data from measurements at 22.63, 75.47, and 100.62 MHz were fitted to spectral densities introduced by Bloembergen, Purcell and Pound (1948), Davidson and Cole (1951), and for the first time, by a new spectral density derived from a Tricomi correlation function recently introduced by Zeidler (1991). For the temperature dependence of the correlation times, a Vogel−Fulcher−Tammann equation was applied. To obtain a reasonable fit with either Bloembergen−Purcell−Pound or Cole−Davidson spectral densities, it was necessary to apply the generalized order parameter from the approach by Lipari and Szabo (1982). The same quality of fit was achieved by the use of the Tricomi spectral density, although in this case it was not necessary to employ the Lipari−Szabo approach.

Introduction

The liquid state of matter is of great importance in nature and technology. Almost all reactions in biological and chemical systems proceed in solution or liquidlike environments. Therefore, it is of interest to develop further the existing models and theories for describing the molecular structure and dynamics of liquids. These models and theories should mediate a better understanding, for example, of the arrangement of the molecules relative to each other or of the dynamic behavior of the molecules and thus of the route of chemical reactions in liquid systems.

Whereas it is often relatively easy to describe the molecular structure and dynamics of the gas or solid state, this is not true for the liquid state. The model that is usually applied for the description of molecular reorientational processes in liquids is the rotational diffusion model. A particularly important experimental method to obtain information on the reorientational dynamics of molecules is the measurement of nuclear spin−lattice relaxation rates. Most of the experimental findings on the reorientation of molecules and molecular segments by means of nuclear relaxation rates were obtained in the extreme narrowing region where the product of the resonance frequency and the reorientational correlation time is much less than unity. Outside the extreme narrowing region, this condition is not valid anymore, and the relaxation rates become frequency-dependent. Bloembergen, Purcell, and Pound[1] employed in their study of relaxation effects on nuclear magnetic resonance phenomena the model of rotational diffusion by Debye.[2]

However, the interpretation of experimental relaxation data with the BPP model by Bloembergen, Purcell, and Pound was often hampered by the fact that the data could not be reproduced with this model when it was assumed that the reorienting molecules or molecular segments behave like totally or partially rigid bodies.[3,4] Thus, it is questionable whether the rotational diffusion model for rigid bodies is suited for the determination

* E-mail: doelle@rwth-aachen.de.

10.1021/jp0208438 CCC: $22.00
Published on Web 11/12/2002

of molecular reorientational dynamics. Hertz[3,4] introduced criteria by which it should be possible to prove the rigidity of the reorienting molecular entities.

To explain the failure of the rotational diffusion model, several other models were developed, many of which were described in the comprehensive review by Beckmann.[5] One of the most successful attempts[5] is the continuous distribution of correlation times by Cole and Davidson,[6] which found broad application in the interpretation of relaxation data from crystalline and glassy solids and viscous liquids. It is, however, a long-standing discussion whether the deviation from the BPP spectral density stems from the fact that there exists a distribution of correlation times or if the correlation functions are just not exponential. At least for highly viscous, glassy systems, the experimental results indicate a distribution of correlation times (cf. to the review by Sillescu[7]), whereas the situation in liquids is still not clear.

Another way to describe the deviations from the BPP spectral density is the so-called model-free approach by Lipari and Szabo,[8] which corresponds to a discrete distribution of correlation times and is a generalization of the two-step model by Wennerström et al.[9] It was originally developed for taking internal motions in macromolecules into account without giving an explicit model when calculating the relaxation data.[10] Although the model-free approach was first applied mainly for the interpretation of relaxation data of macromolecules, it is now also used for fast internal dynamics of small and medium-sized molecules.

It was the aim of the present study to find out by measurements of relaxation data on a model compound also outside the extreme narrowing region whether the rotational diffusion of partially or entirely rigid bodies is in principle applicable to the description of the reorientational motions of molecules or molecular segments in liquids. For such an investigation, a substance had to be found, the molecules of which consist mainly of rigid structural units. The reorientational processes have to be slow enough to leave the extreme narrowing region at experimentally readily accessible temperatures. These requirements are met by the model substance 5,6-dimethyl-1,2,3,4-tetrahydro-1,4-methanonaphthalene[11,12] (5,6-Me_2-THMN, **1**). The neat hydrocarbon **1** is liquid at room temperature and does not crystallize over a wide temperature range. The basic structure of 1,2,3,4-tetrahydro-1,4-methanonaphthalene consists of rigid structural units. The notion "rigid" is used here in accordance with Sykora et al.[13] for molecules or molecular segments consisting of units that cannot perform rotations about single bonds. Their internal motions should be restricted to vibrations about the equilibrium structure. In the study by Dölle and Bluhm,[12] the rotational diffusion was a good model process to describe the anisotropic rotational dynamics of 5,6-Me_2-THMN in neat liquid. In the present study, we investigated whether this also holds outside the extreme narrowing region.

The resonance frequencies of the nuclei are given by the accessible magnetic field strengths via the resonance condition. Since the magnets usually applied for NMR spectroscopy have only fixed field strengths, the correlation times (i.e., the rotational dynamics) have to be varied to leave the extreme narrowing regime. To vary the correlation times and thus also the spectral densities and relaxation data, either the pressure (cf. to the review by Lang and Lüdemann[14]) or the temperature has to be changed. In the present study, ^{13}C spin−lattice relaxation rates and nuclear Overhauser factors in temperature ranges in and outside the extreme narrowing region were measured to observe the temperature dependence of the spectral densities. Subsequently, several models were fitted to the experimental relaxation data.

Theoretical Background

Longitudinal Relaxation of ^{13}C Nuclei. The relaxation of ^{13}C nuclei in medium-sized molecules and for moderate magnetic fields is generally determined by dipolar interactions with directly bonded protons. When the relaxation times are measured under ^{1}H decoupling conditions, the cross relaxation term vanishes,[15] and the intramolecular dipolar longitudinal relaxation rate $(1/T_1^{DD})_i$ for the relaxation of the ^{13}C nucleus i by proton j is related to the molecular reorientations by[15]

$$\left(\frac{1}{T_1^{DD}}\right)_{ij} = \frac{1}{20}(2\pi D_{ij})^2[J(\omega_C - \omega_H) + 3J(\omega_C) + 6J(\omega_C + \omega_H)] \quad (1)$$

with the dipolar coupling constant

$$D_{ij} = \frac{\mu_0}{4\pi}\gamma_C\gamma_H(\hbar/2\pi)r_{ij}^{-3} \quad (2)$$

where μ_0 is the magnetic permeability of the vacuum, γ_C and γ_H are the magnetogyric ratios of the ^{13}C and ^{1}H nuclei, respectively, $\hbar = h/2\pi$ with the Planck constant h, and r_{ij} is the length of the internuclear vector between i and j. The $J(\omega)$ are the spectral densities with the resonance frequencies of the ^{13}C and ^{1}H nuclei, ω_C and ω_H, respectively.

Aromatic ^{13}C nuclei relax even in moderate magnetic fields partially via the chemical-shift anisotropy (CSA) mechanism. The corresponding longitudinal relaxation rate of ^{13}C nucleus i is given by

$$\left(\frac{1}{T_1^{CSA}}\right)_i = \frac{1}{15}\gamma_C{}^2H_0^2(\Delta\sigma_i)^2J(\omega_C) \quad (3)$$

with the magnetic field strength H_0 and the chemical-shift anisotropy $\Delta\sigma = \sigma_{||} - \sigma_\perp$ for an axially symmetric chemical-shift tensor with $\sigma_{||}$ and $\sigma_\perp$ as the components parallel and perpendicular, respectively, to the main principal axis of the chemical-shift tensor.

When discussing the various mechanisms[15] contributing to the ^{13}C relaxation of 5,6-Me_2-THMN, it is reasonable to assume that the aliphatic non-methyl ^{13}C nuclei relax exclusively via the dipolar relaxation mechanism. The experimental relaxation times can then be equated to the dipolar ones, whereas the CSA mechanism also contributes to the relaxation of the aromatic methine ^{13}C nuclei. For the fast rotational motions of small, symmetric molecules or molecular segments such as methyl groups about their symmetry axis, relaxation via the spin−rotation (SR) mechanism also becomes important. Thus, in general, the total longitudinal relaxation rate of ^{13}C nuclei is determined by the relation

$$\left(\frac{1}{T_1}\right)_i = \left(\frac{1}{T_1^{DD}}\right)_i + \left(\frac{1}{T_1^{CSA}}\right)_i + \left(\frac{1}{T_1^{SR}}\right)_i + \dots \quad (4)$$

The nuclear Overhauser (NOE) factor η_i of carbon atom i for relaxation by n_H protons j is given by[15,16]

$$\eta_i = \frac{\gamma_H}{\gamma_C} \frac{\sum_{j=1}^{n_H} \sigma_{ij}}{\sum_{j=1}^{n_H} \rho_{ij} + \rho_i^*} \tag{5}$$

where σ_{ij} is the cross relaxation rate and ρ_{ij} is the dipolar relaxation rate for the interaction between ^{13}C nucleus i and proton j in eq 1. Except the seldom-observed scalar interaction, only the dipolar mechanism contributes to cross relaxation. Therefore, the contributions from all other mechanisms to the relaxation of ^{13}C nucleus i are summarized by the so-called leakage term ρ_i^*, which reduces the NOE factor. Usually, intermolecular dipolar contributions can be neglected for ^{13}C nuclei with directly bonded protons. The contribution of nondirectly bonded protons in the same molecule is also neglected because of the r_{ij} dependence of the relaxation rate.

For the relaxation of ^{13}C exclusively via the intramolecular dipolar interaction, $\rho_i^* = 0$, the NOE factor reaches its maximum value and depends only on the reorientational molecular dynamics:[15,16]

$$\eta_{i,\max} = \frac{\gamma_H}{\gamma_C} \frac{6J(\omega_H + \omega_C) - J(\omega_H - \omega_C)}{J(\omega_H - \omega_C) + 3J(\omega_C) + 6J(\omega_H + \omega_C)} \tag{6}$$

Time Autocorrelation Functions and Spectral Densities.[5] For the case of isotropic liquids, the observed NMR relaxation rates are related after normalization to the molecular dynamics by reduced spectral densities, which are obtained from the reduced correlation functions by Fourier transformation:

$$J(\omega_\lambda, \{x_i\}) = \int_{-\infty}^{\infty} C(t, \{x_i\}) \exp(i\omega_\lambda t)\, dt \tag{7}$$

where ω_λ is the transition frequency and $\{x_i\}$ are the characteristic parameters in the reduced correlation functions $C(t)$. Their time integrals are defined as correlation times τ.

Often a so-called effective correlation time is introduced that contains the different correlation times characterizing the molecular rotational motions such as the correlation times of overall anisotropic rotational diffusion and internal motions. Then, these effective correlation times are in the extreme narrowing case the sum of the single correlation times weighted by structural factors.[15,17,18] In the present study, the effective correlation time is taken to be the area under the reduced correlation function:

$$\tau_{eff} = \int_0^{\infty} \frac{C(t)}{C(0)}\, dt \tag{8}$$

Exponential Correlation Functions and Bloembergen−Purcell−Pound Spectral Density (BPP). When the reorientational motions are of a stochastic (i.e., diffusive) nature and when only one ensemble of reorienting units is present, the correlation functions are given by an exponential function:[5]

$$C_{BPP}(t) = \exp(-t/\tau_{BPP}) \qquad \text{with } t \geq 0 \tag{9}$$

The result of the Fourier transformation for the case of the exponential correlation function is

$$J_{BPP}(\omega_\lambda) = \frac{2\tau_{BPP}}{1 + (\omega_\lambda \tau_{BPP})^2} \tag{10}$$

which corresponds to a Lorentzian function and was used for the first time by Bloembergen, Purcell, and Pound[1] for the interpretation of NMR relaxation data. The parameter τ_{BPP} is the correlation time for rotational diffusion (i.e., for an exponential correlation function). As limiting values are obtained,

$$J_{BPP} = 2\tau_{BPP} \quad \text{for } \omega_\lambda \tau_{BPP} \ll 1 \tag{11}$$

as the extreme narrowing condition, and

$$J_{BPP} = 2\tau_{BPP}^{-1} \omega_\lambda^{-2} \qquad \text{for } \omega_\lambda \tau_{BPP} \gg 1 \tag{12}$$

which is the slow-motion limit. The maximum value is

$$J_{BPP} = \omega_\lambda^{-1} \qquad \text{for } \omega_\lambda \tau_{BPP} = 1 \tag{13}$$

Nonexponential Correlation Functions.[5] For many liquids, especially for viscous liquids and for solids, it was found that the experimental data did not behave like Lorentzian spectral densities. These findings have also been known in the case of nuclear magnetic relaxation data for a long time.[19] Two reasons for such behavior are discussed:

- The rotational motion is not a stochastic process as it was assumed in the preceding section, but it is—at least for some time—correlated. As an example, the cooperative motion in liquid crystals is mentioned here.[20] The result of the cooperative motion is a correlation function that does not decay exponentially. This case is called homogeneous distribution.[21]
- Within an ensemble of reorienting units, subensembles can exist, consisting of molecules for which the rotational dynamics are described by an exponential correlation function and a corresponding Lorentzian spectral density. The characteristic correlation time for each of these subensembles is different, and for the whole ensemble, a heterogeneous distribution of correlation times[21] is found. Such a distribution is assumed for amorphous solids and supercooled liquids, for which a distribution of different surroundings for the rotating units is postulated.

From a formal point of view, one cannot differentiate between both cases,[21] and experimentally, no discrimination is possible by conventional measurements of transversal or longitudinal relaxation data.[22] Quite recently, a number of sophisticated experimental methods have been developed to detect dynamic heterogeneities (cf. to the review by Sillescu[7] and the literature cited therein). Furthermore, several theoretical concepts have been developed to explain the occurrence of the distributions of correlation times.[7]

The correlation functions are related to distributions $\Lambda(\xi, \{x_i\})$ of the correlation times ξ by

$$C(t, \{x_i\}) = \int_0^{\infty} \Lambda(\xi, \{x_i\}) \exp(-t/\xi)\, d\xi \tag{14}$$

in which $\{x_i\}$ is a set of parameters specific for the distribution. The following normalization condition is valid:

$$\int_0^{\infty} \Lambda(\xi, \{x_i\})\, d\xi = 1 \tag{15}$$

The distribution does not depend on the observation frequency; it is a property characteristic for the investigated system. The

corresponding spectral densities are

$$J(\omega, \{x_i\}) = \int_0^\infty \Lambda(\xi, \{x_i\}) \frac{2\xi}{1 + (\omega\tau)^2} \, d\xi \qquad (16)$$

For the BPP spectral density, a distribution consisting of the Dirac δ function is valid:

$$\Lambda_{BPP}(\xi, \tau_{BPP}) = \delta(\xi - \tau_{BPP}) \qquad (17)$$

From this the Lorentzian spectral density is obtained.

Cole−Davidson Spectral Density (CD). The spectral density introduced by Davidson and Cole[6] is given here in the form by Beckmann.[5] The distribution function is

$$\lambda_{CD}(z, \beta) = \begin{cases} \dfrac{\sin(\beta\pi)}{\pi} \left(\dfrac{1}{\exp(-z) - 1} \right)^\beta, & z < 0 \\ 0, & z \geq 0 \end{cases} \qquad (18)$$

where $0 < \beta \leq 1$ and $z = \ln(\xi/\tau_{CD})$ with $\Lambda_{CD}(\xi, \beta) = \lambda_{CD}(z, \beta)/\xi$.[5,23] The correlation function is related to the entire incomplete gamma function γ^*:[24,25]

$$C_{CD} = 1 - \left(\frac{t}{\tau_{CD}} \right)^\beta \gamma^*(\beta, \tau_{CD}, t) \qquad (19)$$

The spectral density is represented in the following closed form:

$$J_{CD}(\omega, \tau_{CD}, \beta) = \frac{2}{\omega} \frac{\sin(\beta \arctan(\omega\tau_{CD}))}{(1 + (\omega\tau_{CD})^2)^{\beta/2}} \qquad (20)$$

The value for $z = 0$ ($\xi = \tau_{CD}$) is called the upper cutoff correlation time; β is a measure of the width of the distribution. The great advantage of the CD distribution is that this analytic result for the spectral density is obtained. According to Dissado and Hill,[26] the occurrence of a spectral density of the CD form indicates that the dynamics are not correlated but show a distribution of activation energies and thus a distribution of correlation times.[5]

The limiting cases are

$$J_{CD}(\omega, \tau_{CD}, \beta) = 2\beta\tau_{CD} \qquad \text{for } \omega\tau_{CD} \ll 1$$

and

$$J_{CD}(\omega, \tau_{CD}, \beta) = 2 \sin(\beta\pi/2) \tau_{CD}^{-\beta} \omega^{-(1+\beta)} \qquad \text{for } \omega\tau_{CD} \gg 1 \qquad (21)$$

whereas the maximum occurs at $\omega\tau \tan(\beta \arctan(\omega\tau_{CD})) = 1$ with a decreasing value of the maximum with decreasing β. In the extreme narrowing region, the CD spectral density is frequency-independent like the BPP spectral density. For $\beta = 1$, the CD spectral density becomes identical to the BPP spectral density.

Another often-used correlation function is the stretched exponential or Kohlrausch−Williams−Watts (KWW) function.[27,28] Within specific limits of the parameter β of the CD function, the parameters τ_{CD} and β can be converted into the corresponding parameters of the KWW distribution.[29,30]

Tricomi Correlation Function (T). Recently, Zeidler[30] proposed the introduction of a more general time-correlation function. This correlation function should possess only two parameters and include the exponential and CD correlation functions as special cases. The generalized correlation function is derived from the Tricomi function[25] and has after normalization the form

$$C_T(t) = \frac{U(\alpha, \beta, \tau_T, t)}{U(\alpha, \beta, \tau_T, 0)} \exp(-t/\tau_T) \qquad (22)$$

where $U(\alpha, \beta, \tau_T, t)$ is the Tricomi function with parameters α and β and the correlation time τ_T. For $\alpha = \beta$, the CD correlation function is obtained, and for $\alpha = \beta = 1$, the Tricomi function is unity and the exponential function is retained. This correlation function can be related to the hypergeometric functions, which are Laplace transformed to give the spectral density of the Tricomi correlation function:

$$J_T(\omega, \tau_T, \alpha, \beta) = 2\tau_T \mathrm{Re}\left\{ (i\omega\tau_T)^{-(1+\beta)} \left(\frac{i\omega\tau_T}{1 + i\omega\tau_T} \right)^\alpha \times \beta \left(B(-\beta, 1 - \alpha + \beta, 1) - B\left(-\beta, 1 - \alpha + \beta, \frac{1}{1 + i\omega\tau_T} \right) \right) \right\} \qquad (23)$$

where Re{...} is the real part of the complex function in brackets and $B(\nu, \mu, x)$ is the incomplete beta function. The limiting cases for this spectral density are given in ref 30.

Model-Free Approach by Lipari and Szabo (LS).[8] For the interpretation of NMR relaxation data of macromolecules, Lipari and Szabo[8] developed a concept for correlation functions and spectral densities that does not make specific assumptions concerning the molecular motions studied. In the case of isotropic overall motion, the total correlation function is completely described by three parameters: the correlation time of the overall molecular motion τ_M, the effective correlation time of the internal motion τ_i, and the generalized order parameter S^2. The latter is a model-free measure for the spatial restriction of the internal motion with $0 \leq S^2 \leq 1$. For $S^2 = 0$, the internal motion is not restricted, but for $S^2 = 1$, it is totally restricted (i.e., it is not taking place). In the latter case, S^2 is an indicator for the fulfillment of one of the rigidity criteria given by Hertz.[3,4] The correlation time τ_i depends on the velocity of the internal motion as well as on its geometry. To interpret the observed relaxation data, the spectral densities are fitted with the above parameters to the experimental data. Afterward, we attempt to relate the obtained parameters to appropriate models.

The correlation function is taken to be the product of the correlation function for the overall reorientation of the molecule and the internal motion:

$$C_{LS}(t) = C_M(t) \, C_i(t) \qquad (24)$$

Assuming that the overall motion is substantially slower than the internal motion, the corresponding spectral density is

$$J_{LS}(\omega, \tau_M, \tau_i, S^2) = S^2 J(\omega, \tau_M) + (1 - S^2) \, J(\omega, \tau_i) \qquad (25)$$

For very fast internal motions, the second term can be neglected, which leaves

$$J_{LS}(\omega) = S^2 J(\omega, \tau_M) \qquad (26)$$

Then, the spectral density is thus not dependent on the correlation time τ_i of internal motion. As motions are very fast compared to the rotational diffusion process, only vibrations have to be considered: stretching vibrations influencing the length

and librations changing the orientation of the bond vectors.[31] The generalized order parameter is divided into two parts:[32,33]

$$S^2 = S_r^2 S_\Omega^2 \tag{27}$$

with the radial and angle-dependent order parameters S_r^2 and S_Ω^2, respectively. Librations always result in a reduction of the spectral density,[31] which cannot be discriminated from a reduction of the coupling constant. Thus, for the dipolar coupling, an apparent elongation of the internuclear vector r_{ij} in the dipolar coupling constant D_{ij} in eq 1 is obtained:[31]

$$r_{\text{eff}} = r_{ij} S^{-1/3} \tag{28}$$

For a model of isotropic overall rotational diffusion with a concurrent fast methyl group rotation, the spectral density from eq 26 can be written as

$$J_{\text{methyl}}(\omega, \tau_M) = \frac{1}{4}(3\cos^2(\Delta) - 1)^2 J(\omega, \tau_M) \tag{29}$$

in which the generalized order parameter is substituted by the model-dependent expression according to Woessner[34] for fast methyl group rotation, where Δ is the angle between the internal rotation axis and the vector connecting the dipolar coupled nuclei.

Although the generalized order parameter was introduced by Lipari and Szabo[8] to describe the internal motions in macromolecules, it will be shown in the present study that this approach can be applied in a much more general sense.

Temperature Dependence of the Correlation Times. Reorientational motions are thermally activated processes. In viscous liquids and glasses, the activation energy seems to increase with decreasing temperature. This behavior is phenomenologically described by the Vogel−Fulcher−Tammann (VFT) equation[35−37]

$$\tau = \tau_{\text{VFT}} \exp\left(\frac{E_{\text{VFT}}}{R(T - T_0)}\right) \tag{30}$$

in which the parameter T_0 is on the order of the glass transition temperature T_g and R is the gas constant. The quantity E_{VFT} is often called an apparent activation energy.

Results

Molecular Geometry. The molecular geometry of hydrocarbon **1** was obtained by calculation with the semiempirical method AM1.[38] It is shown in Figure 1 relative to the principal axis system of inertia.

^{13}C NMR Relaxation. The total longitudinal spin−lattice relaxation rates $1/T_1$ were measured at a ^{13}C resonance frequency of 22.63 MHz in the temperature range from 222 to 328 K, at 75.47 MHz from 303 to 323 K, and at 100.62 MHz from 218 to 328 K; NOE factors η are at 22.63 MHz from 223 to 328 K, at 75.47 MHz from 303 to 323 K, and at 100.62 MHz from 232 to 323 K. The assumed errors in the measurements are smaller than the size of the symbols in the Figures. The experimental data at 22.63 and 100.62 MHz were published in a preliminary study.[39]

Fit of the Different Reorientational Models to the Temperature-Dependent ^{13}C Relaxation Data. To determine the temperature dependence of the ^{13}C relaxation data, we attempted to fit the models for the description of molecular reorientational dynamics introduced in the Theoretical Background section to the experimental data by variations of model-dependent parameters. For this, the BPP, CD, and T spectral densities with or without the LS equations were combined with an Arrhenius or VFT temperature dependence of the effective correlation times. In total, 26 combinations of the above models were tested by simultaneous fits to all experimental ^{13}C relaxation data.

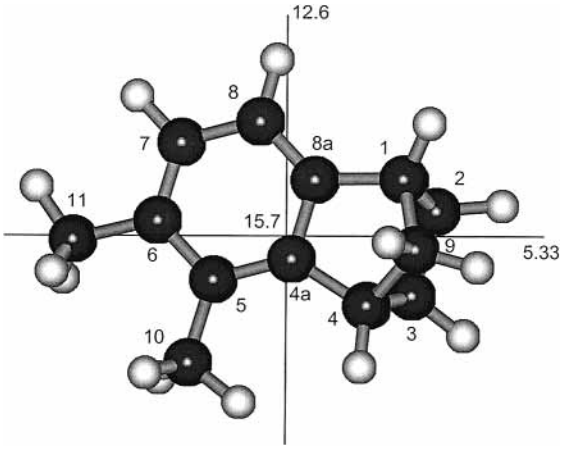

Figure 1. Molecular geometry of 5,6-Me$_2$THMN relative to the principal axis system of inertia and moments of inertia (in 10^{-45} kg m^2).

In the following discussion, only those models are treated in more detail for which a χ^2 value on the order of magnitude of the number of data points was achieved. The value of χ^2 is a measure of the quality of the fit and fulfills the latter criterion for a "good" model.[40] Furthermore, models were rejected that exhibited errors in the parameters larger than 1 order of magnitude than the fitted parameters. Four models were found to fulfill the above criteria:

- the LS/BPP model with a BPP spectral density reduced by the generalized order parameter S^2 according to eqs 10 and 26;
- the LS/CD model with a CD spectral density reduced by S^2 (eqs 20 and 26);
- the LS/C model with a temperature-dependent correlation time τ_M and a temperature-independent constant correlation time τ_i in the BPP spectral densities (eqs 10 and 25); and
- the T model with a Tricomi spectral density (eq 23).

For the temperature dependence of the correlation times, only VFT eq 30 could be used to fit the data since with an Arrhenius equation no satisfactory results were obtained.

The results of the fitted parameters in the different models for the different ^{13}C nuclei in hydrocarbon **1** are given in Table 1. To demonstrate the quality of the fits graphically, the experimental data for aliphatic and aromatic carbon atoms 9 and 7 are compared in Figures 2 and 3, respectively, with the relaxation data obtained from simulation with the parameters in model LS/BPP. The experimental data points for methyl group C10 are compared in Figure 4 to the simulated relaxation data. The data were fitted using the LS/BPP and LS/C models and eq 29 for fast internal rotation with an angle Δ obtained from the geometry optimization given in Table 1. Since the quaternary carbon atoms also relax via the intermolecular dipolar mechanism,[41] which cannot be described adequately, no fit results for them are given here. The effective correlation times obtained from the extreme narrowing region are discussed elsewhere (cf. to ref 42).

Discussion

^{13}C Relaxation Data. As can be seen from Figures 2 to 4, at first the measured relaxation rates increase with decreasing

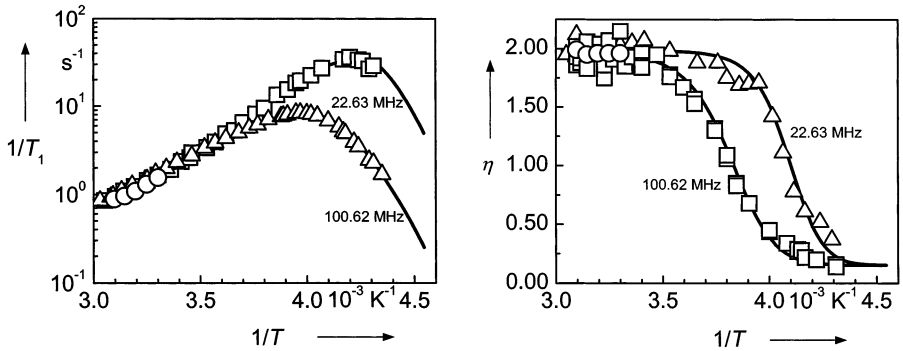

Figure 2. Temperature-dependent experimental longitudinal ^{13}C relaxation rates $1/T_1$ and $\{^1H\}$-^{13}C NOE factors η of aliphatic methylene carbon atom 9 at 22.63 (□), 75.47 (○), and 100.62 MHz (△) compared with the values calculated by means of model LS/BPP.

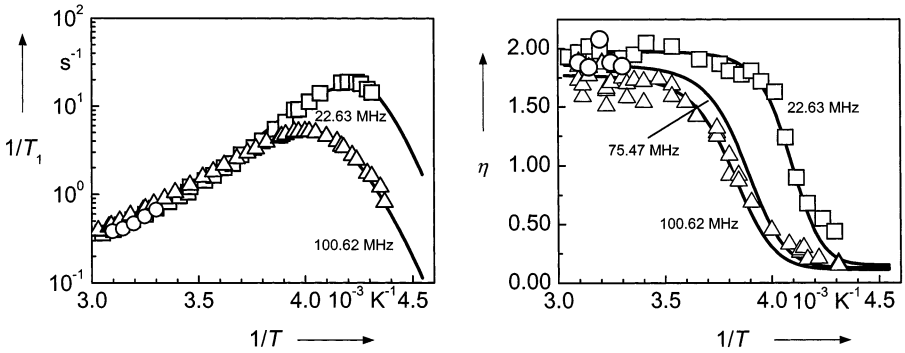

Figure 3. Temperature-dependent experimental longitudinal ^{13}C relaxation rates $1/T_1$ and $\{^1H\}$-^{13}C NOE factors η of aromatic methine carbon atom 7 at 22.63 (□), 75.47 (○), and 100.62 MHz (△) compared with the values calculated by means of model LS/BPP.

TABLE 1: ^{13}C Distances r_{C-H}, Bond Angles Δ, and Number of Data Points *n* Used in the Fit Procedure and Fit Parameters Obtained for Models LS/BPP, LS/CD, LS/C, and T for the Carbon Atoms with Directly Bonded Protons in 5,6-Me_2THMN

carbon atom	1	4	2	3	9	7	8	10	11
r_{C-H}/pm	110.4	110.4	111.5	111.5	111.1	110.1	109.8	111.9	111.9
Δ/°								110.6	110.7
n	147	146	145	145	145	147	147	102	85
					LS/BPP				
χ^2	427	449	401	374	378	538	525	845	680
τ_0/ps	0.54 ± 0.03	0.51 ± 0.03	0.67 ± 0.05	0.67 ± 0.05	0.68 ± 0.05	0.62 ± 0.04	0.51 ± 0.03	0.24 ± 0.04	3.1 ± 0.6
E_{VFT}/kJ mol^{-1}	4.9 ± 0.1	4.9 ± 0.1	4.9 ± 0.1	4.9 ± 0.1	5.0 ± 0.1	4.8 ± 0.1	4.9 ± 0.1	5.9 ± 0.3	3.0 ± 0.3
T_0/K	172 ± 1	172 ± 1	171 ± 1	171 ± 1	169 ± 1	173 ± 1	172 ± 1	164 ± 2	187 ± 3
S^2	0.722 ± 0.006	0.721 ± 0.006	0.719 ± 0.006	0.718 ± 0.006	0.701 ± 0.005	0.659 ± 0.008	0.635 ± 0.008	0.652 ± 0.004	0.735 ± 0.006
Δσ/ppm						213 ± 6	215 ± 6		
					LS/CD				
χ^2	303	326	291	273	338	398	372	610	576
τ_0/ps	1.03 ± 0.08	0.98 ± 0.08	1.13 ± 0.09	1.11 ± 0.09	0.93 ± 0.08	1.3 ± 0.1	1.11 ± 0.09	1.2 ± 0.2	9 ± 2
E_{VFT}/kJ mol^{-1}	4.0 ± 0.1	4.0 ± 0.1	4.2 ± 0.1	4.1 ± 0.1	4.5 ± 0.1	3.8 ± 0.1	3.9 ± 0.1	3.7 ± 0.2	2.0 ± 0.2
T_0/K	183 ± 1	183 ± 1	180 ± 1	180 ± 1	175 ± 1	185 ± 1	185 ± 1	186 ± 2	202 ± 3
S^2	0.80 ± 0.01	0.80 ± 0.01	0.78 ± 0.01	0.78 ± 0.01	0.735 ± 0.008	0.73 ± 0.01	0.71 ± 0.01	0.77 ± 0.01	0.93 ± 0.04
β	0.76 ± 0.02	0.76 ± 0.02	0.80 ± 0.02	0.80 ± 0.02	0.89 ± 0.02	0.75 ± 0.02	0.73 ± 0.02	0.65 ± 0.02	0.53 ± 0.04
Δσ/ppm						222 ± 6	228 ± 6		
					LS/C				
χ^2	356	377	339	321	370	466	427	386	202
τ_0/ps	0.35 ± 0.03	0.33 ± 0.03	0.47 ± 0.04	0.47 ± 0.04	0.60 ± 0.05	0.41 ± 0.03	0.28 ± 0.02	0.23 ± 0.04	1.1 ± 0.3
E_{VFT}/kJ mol^{-1}	5.3 ± 0.1	5.4 ± 0.1	5.3 ± 0.2	5.3 ± 0.1	5.2 ± 0.1	5.3 ± 0.1	5.6 ± 0.1	5.5 ± 0.3	3.8 ± 0.4
T_0/K	169 ± 1	169 ± 1	168 ± 1	168 ± 1	168 ± 1	170 ± 1	167 ± 1	171 ± 2	184 ± 4
S^2	0.713 ± 0.006	0.712 ± 0.006	0.711 ± 0.006	0.711 ± 0.006	0.699 ± 0.006	0.641 ± 0.008	0.612 ± 0.008	0.608 ± 0.005	0.53 ± 0.01
τ_i/ps	13 ± 2	14 ± 2	11 ± 1	10 ± 1	3 ± 1	9 ± 1	11 ± 1	47 ± 2	170 ± 9
Δσ/ppm						226 ± 6	229 ± 6		
					T				
χ^2	351	374	329	314	371	470	429	524	553
τ_0/ps	0.73 ± 0.05	0.70 ± 0.05	0.83 ± 0.06	0.80 ± 0.06	0.73 ± 0.07	0.81 ± 0.05	0.73 ± 0.05	1.5 ± 0.2	8 ± 2
E_{VFT}/kJ mol^{-1}	4.3 ± 0.1	4.3 ± 0.1	4.5 ± 0.1	4.5 ± 0.1	4.9 ± 0.2	4.3 ± 0.1	4.3 ± 0.1	3.3 ± 0.2	2.1 ± 0.2
T_0/K	178 ± 1	178 ± 1	175 ± 1	175 ± 1	171 ± 2	178 ± 1	179 ± 1	190 ± 2	201 ± 3
α	0.983 ± 0.002	0.983 ± 0.002	0.986 ± 0.002	0.987 ± 0.002	0.996 ± 0.001	0.987 ± 0.002	0.982 ± 0.002	0.945 ± 0.005	0.78 ± 0.07
β	0.042 ± 0.006	0.043 ± 0.006	0.035 ± 0.005	0.031 ± 0.005	0.009 ± 0.006	0.023 ± 0.003	0.029 ± 0.003	0.089 ± 0.008	0.29 ± 0.05
Δσ/ppm						221 ± 6	227 ± 6		

temperature or increasing reciprocal temperature, showing the typical behavior in the extreme narrowing region where $\omega\tau \ll 1$ is valid. The reorientational motion becomes slower with decreasing temperature, and the relaxation interactions become more effective. With further increasing reciprocal temperature, a maximum in the longitudinal relaxation rates of **1** is reached:

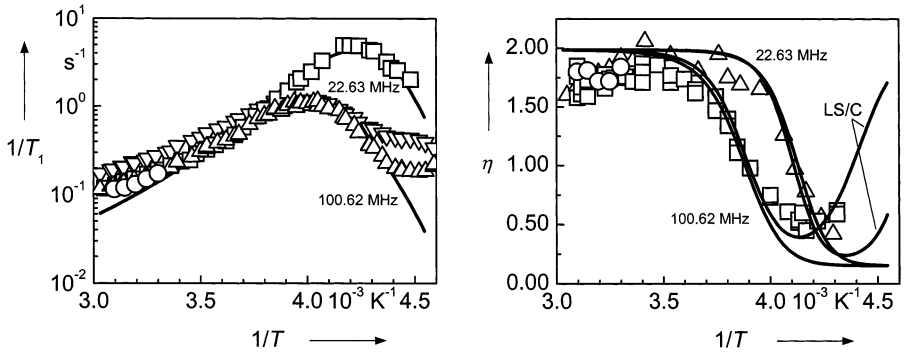

Figure 4. Temperature-dependent experimental longitudinal ^{13}C relaxation rates $1/T_1$ and $\{^1H\}$-^{13}C NOE factors η of methyl carbon atom 10 at 22.63 (□), 75.47 (○), and 100.62 MHz (△) and methyl carbon 11 at 100.62 MHz (▽) compared with the values calculated by means of models LS/BPP and LS/C (for the NOE factors).

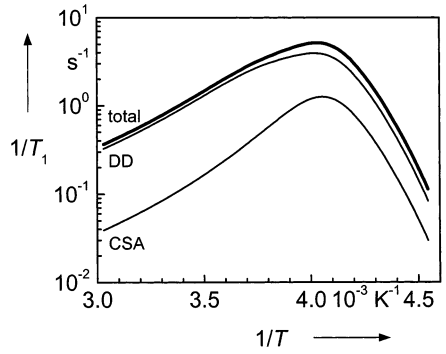

Figure 5. Contributions to the total longitudinal relaxation rate $1/T_1$ resulting from the DD and CSA mechanism for aromatic carbon atom 7 at 100.62 MHz.

for the measuring frequency of 22.63 MHz, the temperature at the maximum lies at about 235 K, and for 100.62 MHz, at 250 K. The relaxation curve is asymmetric, and the absolute value of the slope is increasing with increasing reciprocal temperature, which can be interpreted as a continuous increase of the activation energy in the Arrhenius equation for the relaxation rates. The occurrence of the maximum indicates that the extreme narrowing condition with $\omega\tau \ll 1$ is not valid anymore.

The relaxation rates of the nonaromatic ^{13}C nuclei in the rigid part of the molecule (i.e., excluding the methyl ^{13}C nuclei), when divided by the number of directly bonded protons n_H, were equal to each other for the different measuring frequencies. The relaxation rates of the aromatic ^{13}C nuclei, however, were larger for the higher frequency because of the increasing contribution of the CSA interaction. The relative contributions of the DD and CSA mechanisms to the total longitudinal relaxation rates, which were obtained from the fit parameters in the LS/BPP model (Figure 3), are presented for aromatic ^{13}C nucleus 7 and a ^{13}C measuring frequency of 100.62 MHz in Figure 5 as an example. Even at this relatively high frequency, the CSA mechanism contributes in the extreme narrowing region about 1 order of magnitude less than the DD mechanism.

The relaxation rates of the methyl ^{13}C nuclei divided by the number of directly bonded protons n_H are at all temperatures smaller by a factor of about 10 than the values of the methine and methylene ^{13}C nuclei. This factor corresponds to the value of $(1/4)(3\cos^2(\Delta) - 1)^2 \cong 0.098$, which is obtained from eq 29 for methyl groups with an internal rotation much faster than the overall rotation of the molecule. This factor is part of the rigidity conditions for reorienting molecules or molecular segments by Hertz:[3] When "partially rigid" methyl groups are considered, the relaxation rates of the methyl ^{13}C nuclei are reduced by just this factor compared to the values for the ^{13}C nuclei in the rigid part of the molecule. That means that the reduction of the relaxation rate caused by fast internal methyl rotation was experimentally verified and that the methyl groups can thus be described as partially rigid rotating entities. At even lower temperatures, a second maximum with a value of $[1 - (1/4)(3\cos^2(\Delta) - 1)^2](3/n_H)(1/T_1^{DD}(CH_n))_{max}$ has to be expected, with $(1/T_1^{DD}(CH_n))_{max}$ as the maximum value for the CH_n groups in the rigid aliphatic part of the molecule. This region, however, could not be investigated by the spectrometers used in the present study. As can be seen in Figure 4, the relaxation rates of C11 and C10 in **1** show a shoulder and a minimum, respectively, at 100.62 MHz for a reciprocal temperature of about 4.5×10^{-3} K^{-1}. These features indicate the existence of another faster motional mode (i.e., the internal methyl group rotation) at low temperatures. At high temperatures, the total relaxation rates of the methyl ^{13}C nuclei show a decrease in the slope of the total relaxation rate curve with increasing temperature because of the increasing significance of the SR mechanism.

The NOE factors η of the ^{13}C nuclei of the rigid molecular part were constant at high temperatures and then rapidly decreased at lower temperatures (refer to Figures 2, 3, and 4). The values of the aliphatic ^{13}C nuclei in the rigid molecular frame adopted the limiting value of 1.988 at high temperatures for the extreme narrowing, and at 100.62 MHz and the lowest temperatures, the limiting value of 0.154 for $\omega\tau \gg 1$. Such a temperature dependence of the NOE factors is explained by a slowing down of the reorientational motion and leaving the extreme narrowing region at low temperatures, which is in accordance with the occurrence of the maxima in the relaxation rate−reciprocal temperature curves. The deviation of the NOE factors for the aromatic ^{13}C nuclei from the maximum value of 1.988 in the extreme narrowing region (Figure 3) is caused by the additional relaxation via the CSA mechanism. This is confirmed by the higher relaxation rates of the aromatic ^{13}C nuclei with directly bonded protons. The ratio η/η_{max} is a measure of the contribution of the CSA relaxation mechanism relative to that of the DD mechanism to the total relaxation rate. The dependence of this ratio on the different ^{13}C measuring frequencies is monitored in Figure 6 and was calculated from the same fit parameters as used for Figure 5. The difference between the extreme narrowing region and the slow-motion limit results from the fact that the DD and CSA mechanisms depend differently on the product $\omega\tau$.

The NOE factor for the ^{13}C nuclei of the methyl carbons decreased in the extreme narrowing region with increasing temperature because of the increasing contribution of the SR mechanism, which was particularly significant for C10. Whereas for C11 a maximum value of 1.988 is still reached, this is not

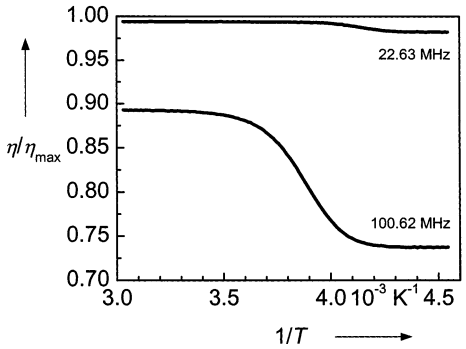

Figure 6. Calculated ratios η/η_{max} for aromatic carbon atom 7 at 22.63 and 100.62 MHz.

true for C10. The smaller NOE value for C10, like the smaller relaxation rate of C10, indicates a faster methyl group rotation than for C11 with the consequence that the SR contribution is higher for C10 and that the dipolar relaxation is less effective relative to the SR mechanism. The NOE factors seem to increase again at 100.62 MHz and the at lowest temperatures because of the fast internal rotation.

Comparison of the Reorientational Models. The models for describing the molecular rotational dynamics that are introduced in the literature[5] have so far mainly been used for the calculation of longitudinal relaxation rates. The experimental data usually deviate from the ideal of the BPP spectral density in two aspects: (1) The maximum value of the experimental relaxation rates is lower than the value calculated from the BPP spectral density. (2) The slope before and after the relaxation-rate maximum (extreme narrowing and slow-motion limit, respectively), when plotting the relaxation rates logarithmically as a function of reciprocal temperature, is not E_A/R and $-E_A/R$ as required for the BPP spectral density with an Arrhenius temperature dependence of the correlation time.

Both aspects are also not fulfilled in the present investigation. The second point showed up in the form of an apparent continuous increase of the activation energy with decreasing temperature. This behavior was well described by VFT eq 30. The T_0 values in Table 1 range from 167 to 185 K for the ^{13}C nuclei of the rigid molecular part. From measurements of the viscosities, a T_0 of (192 ± 5) K was obtained. These T_0 values correspond to a glass-transition temperature T_g of 188 K at atmospheric pressure observed by Reuter et al.[43] from differential thermal analyses. 5,6-Me_2THMN has to be classified as a "fragile" organic glass-forming liquid because of its intermolecular interactions and the temperature dependence of its reorientational motion and viscosities.[44]

Another criterion that the models have to fulfill becomes obvious in Figures 2 and 4: The dipolar relaxation rates calculated from the model must not be frequency-dependent in the extreme narrowing region. The latter was true for all models applied in the present study. The χ^2 values in Table 1 demonstrate that the four models describe the experimental relaxation data approximately equally well. The magnitude of the χ^2 values also shows that all four models can be used for modeling the data because the values all have the same order of magnitude as the number of data points.[40] This statement is corroborated by the graphical comparison of the experimental relaxation data with those calculated by the models (Figures 2 to 4). Only the results for model LS/BPP (and LS/C for the NOE factors of methyl carbon 10) are shown since the results for the other models do not differ much in the temperature range observed. Although in models LS/CD, LS/C, and T an additional parameter compared to the LS/BPP model was introduced, the improvement in the χ^2 values was not dramatic. Except for the relaxation of the methyl ^{13}C nuclei, the best fit was obtained with the LS/CD model, followed by the LS/C and T models. For the methyl group ^{13}C nuclei, model LS/C was best, followed by model T and then model LS/CD.

The temperature-independent correlation times τ_i obtained from the model LS/C were for high temperatures of the same order of magnitude as the overall rotational correlation times τ_M. Attempts to fit models with temperature-dependent correlation times τ_i were not successful. One possible reason for this finding is that the correlation times τ_i represent a fast decay in the correlation function (refer to the discussion of Figure 9 below) for which it is not important what the temperature dependence is provided it exhibits the short-time behavior within a time interval before the onset of the relatively slow rotational diffusion regime. To be able to model the possible temperature dependence of these correlation times, measurements at much higher frequencies would be necessary. Another reason could be that these correlation times are in fact not temperature-dependent or only weakly temperature-dependent in the observed temperature interval. Clore et al.[45] observed similar results when interpreting relaxation data of proteins with an extended model-free approach. These authors also obtained correlation times from the fits to the experimental data, which corresponded to motions on a similar time scale as the reorientational correlation times. Schurr et al.,[46] however, tested in a simulation the extended model and found slow-motional modes for single molecular segments concurrent with an improvement of the quality of the fit, although the input data of the simulation did not contain slow-motional modes.

In some cases, the generalized order parameters S^2 were also found to be slightly temperature-dependent (i.e., a decreasing S^2 was observed with increasing temperature in studies of carbohydrates).[47−50] Thus, models with a temperature-dependent S^2 were employed for fitting the data; however, it was not possible to obtain reasonable fits with these models. This result could either mean that no temperature dependence exists in the case of the 5,6-Me_2THMN or that it is too weak to be fitted properly. Furthermore, no models for the temperature dependence of the order parameters, which could be adopted in the models for the spectral density, were found in the literature.

When comparing the fit parameters in Table 1 for the aliphatic carbon atoms within each model, it turns out that the parameters correspond to each other very well. The small differences between the values of carbons C1 and C4 on one hand and C2, C3, and C9 on the other hand can be explained by the anisotropy of the molecular rotational motion. The vectors of C1 and C4 are oriented approximately perpendicular to those of C2, C3, and C9. The anisotropy of the reorientational motion of 5,6-Me_2THMN and its temperature dependence was studied by the present author as well and will be dealt with in a forthcoming publication. Here, it should be mentioned only that the activation parameters for the rotational diffusion constants about the three axes in space are quite similar and thus would not influence the findings in the present study concerning the spectral densities. Furthermore, from simulations of the spectral densities, it is known that the anisotropies have to be quite large to show effects on the spectral densities, such as shoulders or even separate maxima, which was not observed in the case of 5,6-Me_2THMN.

The χ^2 values for the aromatic ^{13}C nuclei of C7 and C8 are slightly increased compared to those of the aliphatic carbons of the rigid molecular moiety. The fit parameters compare quite well with those of the latter carbon atoms. The absolute value

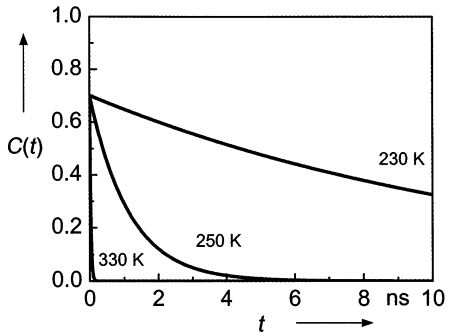

Figure 7. Correlation function $C(t)$ for aliphatic methylene carbon atom 9 calculated for model LS/BPP at different temperatures.

of the chemical-shift anisotropy $|\Delta\sigma|$ is similar to that found for benzene of about 183 ppm.[51] The ratio η/η_{max} calculated from the experimental NOE factors in the extreme narrowing regime was 0.88 at 100.62 MHz, being identical within the error limits to the value of 0.89 obtained from the fit (refer also to Figure 6).

Almost all data points for methyl carbons C10 and C11 correspond to that part of the relaxation curve that results mainly from the slow overall motion of the molecule and therefore the internal rotation axis C−CH_3. However, the fit parameters in Table 1 match only approximately those obtained for the ^{13}C nuclei of the rigid molecular frame, and the χ^2 values for the fit of the methyl carbons are significantly larger than for the fit of the rigid-frame carbon atoms. This might be a consequence of the fact that the spin relaxation, which results from the fast internal rotation of the methyl groups, superimposes the relaxation from the slow overall motion, becoming particularly evident for methyl carbon C11, which exhibits a shoulder at 100.62 MHz and 4.5×10^{-3} K^{-1} (Figure 4). The data points for the methyl groups in the high-temperature region above 293 K could not be described by the equations for the dipolar relaxation because of the additional contribution from the spin−rotation relaxation mechanism. Thus, these data as well as those at temperatures below the minimum of the relaxation curve for C10 and the shoulder for C11 were excluded in the fit of the data.

In an earlier study by Schlenz et al.,[39] the temperature dependence of the relaxation data of **1** was fitted to the experimental data at 22.63 and 100.62 MHz. However, the fits were performed only for single data sets of relaxation rates at a single frequency. The observed frequency dependence was explained by the fact that the data at 22.63 MHz could not be measured at low enough temperatures.[39] These arguments now find subsequent confirmation since the fit parameters for model LS/BPP in Table 1 of the present investigation are within the error limits, in very good accordance with the values by Schlenz et al. (model VFT/C in ref 39). It is emphasized here that the fit parameters of the present investigation were obtained by simultaneous fitting to all ^{13}C longitudinal relaxation rates and NOE factors of the respective carbon atom.

After having determined the fit parameters, it was possible to simulate the corresponding time autocorrelation functions and the related spectral densities with these parameters by means of the equations given above. As the results for the correlation functions do not differ much from the appearance of the simple exponential function in the LS/BPP model, only the results for this model are shown in Figure 7 for the lowest and highest measured temperatures of about 230 and 330 K, respectively, and the temperature of 250 K, where the maximum in the relaxation curve approximately appears for the measuring frequency of 100.62 MHz. Multiplication by the order parameter S^2 reduces the correlation function just by this factor so that it starts at S^2 instead of unity.

In Figure 8, the spectral densities are compared to each other for models LS/BPP, LS/CD, LS/C, and T and temperatures 230, 250, and 330 K. It is obvious that the spectral densities for models LS/BPP and LS/CD do not differ much from each other, whereas those for models LS/C and T differ significantly in the high-frequency region above 10^9 s^{-1}. The common feature of both latter spectral densities is that the curves for the different temperatures come closer to each other with increasing frequen-

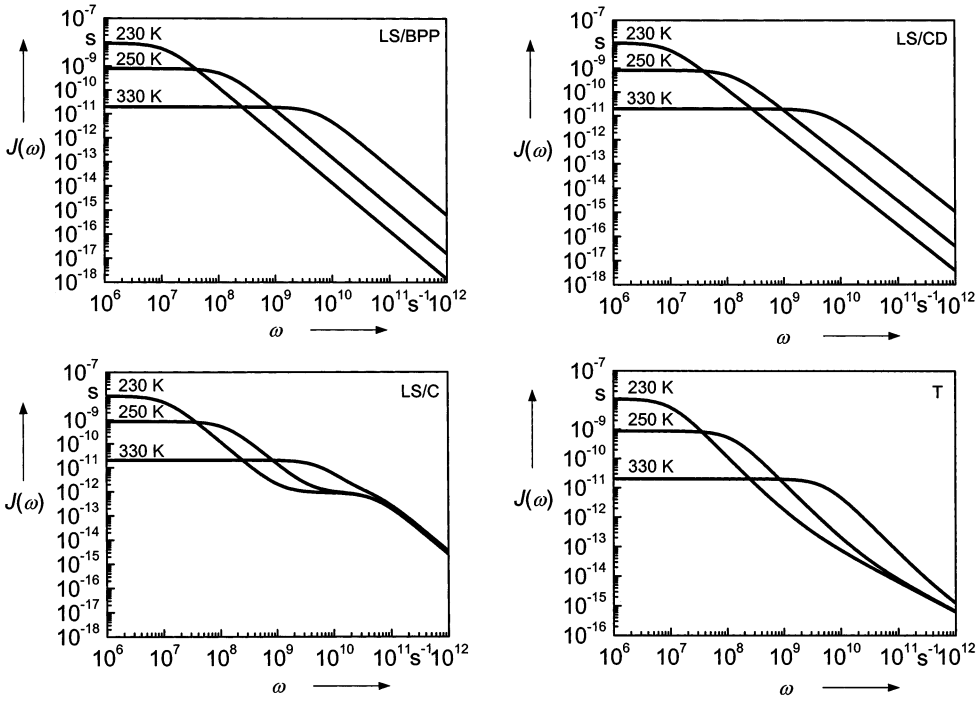

Figure 8. Spectral densities $J(\omega)$ for aliphatic methylene carbon atom 9 calculated for models LS/BPP, LS/CD, LS/C, and T at different temperatures.

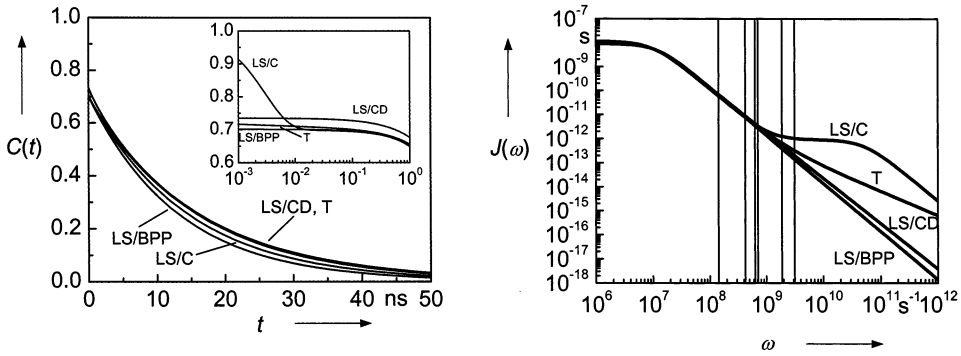

Figure 9. Comparison of the correlation functions $C(t)$ and spectral densities $J(\omega)$ for aliphatic methylene carbon atom 9 calculated for models LS/BPP, LS/CD, LS/C, and T for a temperature of 230 K. The vertical lines indicate the angular measuring frequencies.

cies. The spectral density of the LS/C model forms a plateau that is differently pronounced for the different temperatures. To estimate the significance of these differences in the spectral densities for the modeling of relaxation data, in Figure 9, the spectral densities of all models are compared to each other for 230 K because the differences are most prominent at the lowest measured temperatures. The positions of the angular frequencies ω_C, $\omega_C - \omega_H$, and $\omega_C + \omega_H$, which were sampled according to the idea of spectral density mapping by Peng and Wagner,[52] are also indicated in Figure 9. It is evident that the differences in the spectral densities, even at this lowest temperature, become effective only for the highest sampled frequencies.

The related correlation functions are also given in Figure 9. The inset in Figure 9 exhibits the behavior of the correlation functions at very short times between 1 ps and 1 ns compared to the time scale of molecular rotational motion with correlation times on the order of 0.1 ns. The short times of the correlation functions correspond to the high-frequency region of the spectral densities between 10^9 and 10^{12} s^{-1}. As already mentioned, the correlation functions do not differ much for the different models. One interesting feature, however, is shown by the curve for model LS/C: Its correlation function decreases quickly to the value of the generalized order parameter before the time regime of rotational diffusion is reached, at a time on the order of 10 ps, which reproduces approximately the value of the correlation time τ_i.

Interpretation of the Reduction in the Spectral Density. The reduction of the spectral density is common for all applied models, and in the following discussion, an explanation of the meaning of this reduction will be given. Henry and Szabo[31] investigated the influence of vibrations on the line shapes of solid-state spectra and relaxation. Ultrafast motions of C−H bonds such as stretching and bending vibrations affect the effective C−H bond distances and therefore also the dipolar coupling constant D_{ij} in eq 1. The contribution of stretching vibrations is almost independent of temperature and molecular structure because it results almost exclusively from the zero-point vibrations of the molecules. Furthermore, its contribution to the effective bond length in eq 28 is relatively small because of the opposite signs of the harmonic and anharmonic terms. For propane and octane in the gas phase, changes in the bond lengths on the order of 1.0% were found.[31] The values for contributions from librations of the C−H bonds in these flexible molecules were on the order of 1.3 and 4.6%, respectively. Dill and Allerhand[53] quote a value of 1 to 2% for the bond elongation by vibrations. Kowalewski et al.[54] found in their NMR relaxation study on the dipolar $^{13}C-^{1}H$ coupling constant in dissolved hexamethylenetetramine an effective bond length that is 4.1% larger than the one from neutron-scattering experiments.

In the present investigation, an average reduction of the spectral density by approximately 30% was observed, which is equivalent to a generalized order parameter S^2 of 0.70 in the LS/BPP and LS/C models. This corresponds to an effective bond length that is larger by approximately 6% than the equilibrium bond length calculated in the semiempirical geometry optimization. Such a big difference cannot be explained in the case of the rigid structure of molecule **1** only by the occurrence of vibrations since for the flexible propane a total elongation of 2.3% was found. The result for the aromatic $^{13}C-^{1}H$ bonds in **1** can directly be compared to values for benzene from a recent study by Hardy et al.:[55] Here, the harmonic contribution of +0.6% (stretching, −1.0% and bending, +1.6%) and the anharmonic contribution of +1.9% result in a total elongation of 2.5% compared to an elongation observed in the NMR relaxation experiments for the aromatic $^{13}C-^{1}H$ bonds of about 7% when the average S^2 is 0.65 for the aromatic ^{13}C nuclei. Similar reasoning should be true for the other direct C−H bonds in the molecule.

Thus, it is concluded that the additional elongation is a consequence of the dynamic behavior of the molecule as a whole (i.e., the entire molecule performs ultrafast librations in the cage of the surrounding liquid, followed by the rotational motions on the rotational diffusion time scale). Thus, a fast process precedes the relatively slow diffusive motion, which results in a fast decay of the reorientational autocorrelation function before the diffusive process starts. This fast motion causes the observed reduction in the spectral density, which cannot be directly detected by measurements of NMR relaxation data in the usually accessible temperature and frequency range and that manifests itself in the missing part of the BPP spectral density. The generalized order parameter includes not only the intramolecular contributions for vibrations and librations according to eq 27 but also contributions that are a consequence of librations of the whole molecule in the potential of the cage of the surrounding particles in the liquid. Therefore, the equation has to be extended by a kind of "intermolecular" term:

$$S^2 = (S_r^2 S_\Omega^2)_{intra}(S_\Omega^2)_{inter} \tag{31}$$

Interestingly, this feature of the fast decay of the correlation function before the onset of the rotational diffusion is exhibited by the LS/C model (refer to Figure 9).

The order parameter such defined represents a more general form for describing the influence of dynamic processes on the observed coupling constants. So far the generalized order parameter was applied in the literature for describing fast internal motions only, the purpose for which it was originally introduced by Lipari and Szabo.[8]

Conclusions

When considering the relaxation data that were obtained for model compound 5,6-Me_2THMN not only in the extreme narrowing regime, it becomes evident that the molecular reorientational dynamics cannot be exclusively described by a diffusive process of rigid bodies since the BPP spectral density[1] obtained from a rotational diffusion process does not reproduce the data adequately. Four models of spectral densities were found that describe the data very well in the studied temperature and frequency ranges. Model LS/BPP by Lipari and Szabo[8] combined with a BPP spectral density has the advantage of being conceptually simple and of requiring the least number of fit parameters, whereas the more sophisticated models might gain importance for measurements at lower temperatures or higher magnetic fields. The physical meaning of the parameters in the Tricomi spectral density, which was applied for the first time in the present investigation for the interpretation of NMR relaxation data, is not yet known.

In the literature, the reduction of the spectral density was related to fast internal motions, which was confirmed for proteins by molecular dynamics (MD) simulations or normal coordinate analysis.[32,33,56−59] The effect of molecular motions on the accuracy of determining molecular distances was recently studied for two model peptides by Abseher et al.[60] Part of the reduction in the spectral density observed in the present study of hydrocarbon 5,6-Me_2THMN by an average generalized order parameter of 0.70 (for the LS/BPP model) was attributed to librations of the entire molecule in its surrounding cage of liquid molecules. For small molecules, such dynamic behavior is already known from MD simulations[61−65] or from performing optical Kerr effect measurements (refer, for example, to Ricci et al.[66]). This process appears to be a general feature, being characteristic for the dynamics of small and medium-sized molecules in liquids leading to a reduction of the spectral density or an apparent reduction of the dipolar coupling constant.

In the present study, the generalized order parameter was for the first time split into intra- and intermolecular terms. When for the intramolecular term $(S^2)_{intra}$ a value of 0.86 is assumed, corresponding to 2.5% bond elongation resulting from internal motions,[31] a value of about 0.81 is obtained for $(S^2)_{inter}$, being 0.76 in the case of the aromatic C−H bonds. The reorientational dynamics of large molecules such as proteins is much slower compared to the dynamics of the surrounding (solvent) molecules, resulting in a more hydrodynamiclike motion damped by the friction with the solvent molecules. Compared to that, the reorientation of small and medium-sized molecules such as 5,6-Me_2THMN surrounded by molecules of the same size in neat liquids or of a similar size in solutions is much less damped. Thus, it can be assumed that the contribution to the order parameter from the intramolecular term predominates the intermolecular term for large molecules such as proteins dissolved in solvents with molecules of a relatively small size.

The reduction of the spectral density results in larger reorientational correlation times obtained in the fit. Therefore, the correlation times determined by Dölle and Bluhm[12] from relaxation data in the extreme narrowing regime are too small by a factor of approximately 0.70. This finding has a general consequence for the determination of molecular structures and reorientational dynamics: As long as the reduction of the spectral density caused by fast internal or overall molecular dynamics is not known from measurements outside the extreme narrowing region, no reliable quantitative statements about the velocity of the rotational diffusion process can be made, and the diffusion model is of only qualitative value for the interpretation of the data.[61] Thus, it is necessary to employ modified spectral densities such as those introduced in the present study or the representation of the reorientational correlation functions by other means such as the cumulant expansion.[62−64,67] Furthermore, the determination of exact structural data calculated from measurements of dipolar coupling constants is also hindered by this fact. It should be emphasized here that the observed elongation of bond lengths from equilibrium distances to effective distances is a result of dynamic effects, part of which are characteristic for the special nature of dynamics in liquids.

Methods

^{13}C NMR Relaxation Data. The measurements at a ^{13}C resonance frequency of 75.47 MHz were performed on a Bruker CXP 300 spectrometer (B_0 = 7.047 T, $\nu_0(^{13}C)$ = 75.47 MHz, $\nu_0(^1H)$ = 300.13 MHz, lock on ^{2}H in a deuterated solvent in a 10-mm NMR tube surrounding the inner NMR tube with 7.5-mm diameter containing 5,6-Me-THMN). The spin−lattice relaxation times were measured using the inversion−recovery pulse sequence and were calculated from the ^{1}H broadband decoupled ^{13}C spectra by a three-parameter exponential fit implemented in the spectrometer software. The relaxation data were extracted from signal heights. The measurements of the spin−lattice relaxation times were repeated at least 5 times, those for the NOE factors, 10 times, and then the average values were calculated. The mean standard deviations of the mean experimental data for the NOE factors were always smaller than the scatter of the average values about the maximum value of the NOE factor of 1.988 for pure dipolar relaxation in the extreme narrowing regime. Thus, for the evaluation of the data, the (larger) error value given below was assumed (see below). The relaxation of the methyl ^{13}C nuclei becomes increasingly affected by the SR mechanism at higher temperatures. Therefore, these data points, which deviated from the curves calculated for the dipolar mechanism, were omitted from the fitting of the data with the reorientational models. The error in the temperature was estimated to be ±1 K. For the measurements at 22.63 and 100.62 MHz and further experimental details, refer to refs 11 and 39.

Evaluation of the Reorientational Models. For the computational data evaluation, FORTRAN90 programs were used that were run on IBM-compatible computers. A χ^2 fit of the reorientational models with the corresponding model parameters to the experimental relaxation data of the respective ^{13}C nucleus was performed for the different frequencies simultaneously by employing the Levenberg−Marquardt method.[40] For the fit procedure, an average error for the experimental data was estimated, namely, 10% for the NOE factors at 22.63 and 100.62 MHz, 5% for the longitudinal relaxation rates at 22.63 MHz and NOE factors at 75.47 MHz, and 3% for the longitudinal relaxation rates at 75.47 and 100.62 MHz. The correlation functions of eqs 19 and 22 and the spectral density of eq 23 were computed using equations and algorithms given in ref 25.

Acknowledgment. This paper is dedicated to Professor M. D. Zeidler on the occasion of his 65th birthday. Financial support by the Deutsche Forschungsgemeinschaft and the Fonds der Chemischen Industrie is gratefully acknowledged. I thank M. D. Zeidler for many helpful discussions and his support of this work and one of the reviewers for clarifying comments, which resulted in an improvement of the manuscript.

References and Notes

(1) Bloembergen, N.; Purcell, E. M.; Pound, R. V. *Phys. Rev.* **1948**, *73*, 679.
(2) Debye, P. *Polare Molekeln*; Verlag von S. Hirzel: Leipzig, Germany, 1929.
(3) Hertz, H. G. *Prog. Nucl. Magn. Reson. Spectrosc.* **1983**, *16*, 115.
(4) Hertz, H. G. *Lect. Notes Phys.* **1987**, *293*, 41.
(5) Beckmann, P. A. *Phys. Rep.* **1988**, *171*, 85.
(6) Davidson, D. W.; Cole, R. H. *J. Chem. Phys.* **1951**, *19*, 1484.
(7) Sillescu, H. *J. Non-Cryst. Solids* **1999**, *243*, 81.
(8) Lipari, G.; Szabo, A. *J. Am. Chem. Soc.* **1982**, *104*, 4546.
(9) Wennerström, H.; Lindman, B.; Söderman, O.; Drakenberg, T.; Rosenholm, J. B. *J. Am. Chem. Soc.* **1979**, *101*, 6860.
(10) Lipari, G.; Szabo, A. *J. Am. Chem. Soc.* **1982**, *104*, 4559.
(11) Dölle, A.; Bluhm, T. *J. Chem. Soc., Perkin Trans. 2* **1985**, 1785.
(12) Dölle, A.; Bluhm, T. *Mol. Phys.* **1986**, *59*, 721.
(13) Sykora, S.; Vogt, J.; Bösiger, H.; Diehl, P. *J. Magn. Reson.* **1979**, *36*, 53.
(14) Lang, E. W.; Lüdemann, H.-D. *Prog. Nucl. Magn. Reson. Spectrosc.* **1993**, *25*, 507.
(15) Lyerla, J. R.; Levy, G. C. *Top. Carbon-13 NMR Spectrosc.* **1972**, *1*, 79.
(16) Neuhaus, D.; Williamson, M. *The Nuclear Overhauser Effect in Structural and Conformational Analysis*; VCH Publishers: New York, 1989.
(17) Spiess, H. W. Rotation of Molecules and Nuclear Spin Relaxation. In *NMR*: *Basic Principles and Progress*; Diehl, P., Fluck, E., Kosfeld, R., Eds. Springer-Verlag: Berlin, 1978; Vol. 15.
(18) Vold, R. L.; Vold, R. R. *Prog. Nucl. Magn. Reson. Spectrosc.* **1978**, *12*, 79.
(19) Gutowsky, H. S.; Saika, A.; Takeda, M.; Woessner, D. E. *J. Chem. Phys.* **1957**, *27*, 534.
(20) Freed, J. H. *J. Chem. Phys.* **1977**, *66*, 4183.
(21) Kaplan, J. I.; Garroway, A. N. *J. Magn. Reson.* **1982**, *49*, 464.
(22) Rössler, E; Sillescu, H. *Chem. Phys. Lett.* **1984**, *112*, 94.
(23) Connor, M. T. *Trans. Faraday Soc.* **1964**, *60*, 1574.
(24) Albayrak, C.; Zeidler, M. D.; Küchler, R; Kanert, O. *Ber. Bunsen-Ges. Phys. Chem.* **1989**, *93*, 1119.
(25) Spanier, J; Oldham, K. B. *An Atlas of Functions*; Hemisphere Publishing Corporation: Washington, DC, 1987.
(26) Dissado, L. A; Hill, R. M. *Nature (London)* **1979**, *279*, 685.
(27) Kohlrausch, F. *Pogg. Ann.* **1863**, *119*, 337.
(28) Williams, G.; Watts, D. C. *Trans. Faraday Soc.* **1970**, *66*, 80.
(29) Lindsey, C. P.; Patterson, G. D. *J. Chem. Phys.* **1980**, *73*, 3348.
(30) Zeidler, M. D. *Ber. Bunsen-Ges. Phys. Chem.* **1991**, *95*, 971.
(31) Henry, E. R; Szabo, A. *J. Chem. Phys.* **1985**, *82*, 4753.
(32) Brüschweiler, R.; Roux, B.; Blackledge, M.; Griesinger, C.; Karplus, M; Ernst, R. R. *J. Am. Chem. Soc.* **1992**, *114*, 2289.
(33) Brüschweiler, R. *J. Am. Chem. Soc.* **1992**, *114*, 5341.
(34) Woessner, D. E. *J. Chem. Phys.* **1962**, *36*, 1.
(35) Vogel, H. *Phys. Z.* **1921**, *22*, 645.
(36) Fulcher, G. *J. Am. Ceram. Soc.* **1925**, *8*, 339.
(37) Tammann, G; Hesse, W. *Z. Anorg. Allg. Chem.* **1926**, *156*, 245.
(38) Dewar, M. J.; Zoebisch, E. G.; Healy, E. F.; Stewart, J. J. P. *J. Am. Chem. Soc.* **1985**, *107*, 3902.
(39) Schlenz, U.; Dölle, A.; Hertz, H. G. *Z. Naturforsch., A: Phys. Sci.* **1995**, *50*, 631.
(40) Press, W. H.; Flannery, B. P.; Teukolsky, S. A.; Vetterling, W. T. *Numerical Recipes: The Art of Scientific Computing*; Cambridge University Press: Cambridge, U.K., 1989.
(41) Dölle, A. *J. Magn. Reson., Ser. A* **1995**, *114*, 258.
(42) Gruhlke, P.; Dölle, A. *J. Chem. Soc., Perkin Trans. 2* **1998**, 2159.
(43) Reuter, J.; Brückert, T.; Würflinger, A. *Z. Naturforsch., A: Phys. Sci.* **1993**, *48*, 705.
(44) Elliott, S. R. *Physics of Amorphous Materials*, 2nd ed.; Longman Scientific & Technical: Harlow, U.K., 1990.
(45) Clore, G. M.; Szabo, A.; Bax, A.; Kay, L. E.; Driscoll, P. C.; Gronenborn, A. M. *J. Am. Chem. Soc.* **1990**, *112*, 4989.
(46) Schurr, J. M.; Babcock, H. P.; Fujimoto, B. S. *J. Magn. Reson., Ser. B* **1994**, *105*, 21.
(47) McCain, D. C.; Markley, J. L. *J. Magn. Reson.* **1987**, *73*, 244.
(48) Kowalewski, J.; Widmalm, G. *J. Phys. Chem.* **1994**, *98*, 28.
(49) Mäler, L.; Widmalm, G.; Kowalewski, J. *J. Phys. Chem.* **1996**, *100*, 17103.
(50) Effemey, M.; Lang, J.; Kowalewski, J. *Magn. Reson. Chem.* **2000**, *38*, 1012.
(51) Fung, B. M.; Parhami, P. *J. Magn. Reson.* **1985**, *63*, 168.
(52) Peng, J. W.; Wagner, G. *J. Magn. Reson.* **1992**, *98*, 308.
(53) Dill, K.; Allerhand, A. *J. Am. Chem. Soc.* **1979**, *101*, 4376.
(54) Kowalewski, J.; Effemey, M.; Jokisaari, J. Personal communication.
(55) Hardy, E. H.; Merkling, P. J.; Witt, R.; Dölle, A. *Z. Phys. Chem.* **2000**, *214*, 1687.
(56) Levy, R. M.; Karplus, M.; McCammon, J. A. *J. Am. Chem. Soc.* **1981**, *103*, 994.
(57) Brüschweiler, R.; Case, D. A. *Phys. Rev. Lett.* **1994**, *72*, 940.
(58) Kieffer, B.; Koehl, P.; Lefevre, J. F. *Biochimie* **1992**, *74*, 815.
(59) Balasubramanian, S.; Nirmala, R.; Beveridge, D. L.; Bolton, P. H. *J. Magn. Reson.* **1994**, *104*, 240.
(60) Abseher, R.; Lüdemann, S.; Schreiber, H.; Steinhauser, O. *J. Am. Chem. Soc.* **1994**, *116*, 4006.
(61) Kovacs, H.; Kowalewski, J.; Laaksonen, A. *J. Phys. Chem.* **1990**, *94*, 7378.
(62) Lynden-Bell, R. M.; Steele, W. A. *J. Phys. Chem.* **1984**, *88*, 6514.
(63) Lynden-Bell, R. M.; McDonald, I. R. *Mol. Phys.* **1981**, *43*, 1429.
(64) Böhm, H. J.; Lynden-Bell, R. M.; Madden, P. A.; McDonald, I. R. *Mol. Phys.* **1984**, *51*, 761.
(65) Chelli, R.; Cardini, G.; Ricci, M.; Bartolini, P.; Righini, R.; Califano, S. *Phys. Chem. Chem. Phys.* **2001**, *3*, 2803.
(66) Ricci, M.; Bartolini, P.; Chelli, R.; Cardini, G.; Califano, S.; Righini, R. *Phys. Chem. Chem. Phys.* **2001**, *3*, 2795.
(67) Gburski, Z.; Stassen, H.; Kachel, A.; Dorfmüller, T. *J. Mol. Struct.* **1997**, *410*−*411*, 503.